Localization of Interacting Dirac Fermions

Tianxing Ma,[1,2] Lufeng Zhang,[1] Chia-Chen Chang,[3,*] Hsiang-Hsuan Hung,[4] and Richard T. Scalettar[3]
[1]Department of Physics, Beijing Normal University, Beijing 100875, China
[2]Beijing Computational Science Research Center, Beijing 100193, China
[3]Department of Physics, University of California, Davis, California 95616, USA
[4]Department of Physics, The University of Texas at Austin, Austin, Texas 78712, USA

(Received 25 April 2017; revised manuscript received 18 December 2017; published 12 March 2018)

Using exact quantum Monte Carlo calculations, we examine the interplay between localization of electronic states driven by many-body correlations and that by randomness in a two-dimensional system featuring linearly vanishing density of states at the Fermi level. A novel disorder-induced nonmagnetic insulating phase is found to emerge from the zero-temperature quantum critical point separating a semimetal and a Mott insulator. Within this phase, a phase transition from a gapless Anderson-like insulator to a gapped Mott-like insulator is identified. Implications of the phase diagram are also discussed.

DOI: 10.1103/PhysRevLett.120.116601

Introduction—In disordered low-dimensional noninteracting systems, single-particle eigenstates are exponentially localized due to coherent backscattering [1]. Over the last decade, the study of correlation effects on disordered, noninteracting Anderson insulators has witnessed an extraordinary development [2,3]. In particular, the concept of many-body localization [4] has received much attention, and profoundly extended our pictures of the metal-insulator transitions to many fundamental nonequilibrium questions such as eigenstate thermalization [3].

In a second noninteracting context, free fermions on a honeycomb lattice, the discovery of topological insulators [5,6] has further enriched our understanding of matters by going beyond Landau's symmetry breaking theory. A current frontier of theoretical research focuses on expanding the phenomenon to correlated systems [7,8]. Remarkable results with implications outside condensed matter physics have been reported. For example, topological superconductors [6] have been shown to display fascinating properties including the emergence of space-time supersymmetry [9–11].

Since disorder and interactions are both present in real materials, it is natural to put these two new areas together and investigate the role of correlations on a disordered Dirac system. Study of this problem in the case of attractive interactions has already led to the interesting conclusion that disorder induces a superconducting phase by giving rise to a nonzero density of states [12]. In this Letter we address the important questions which arise when *repulsive* interactions and randomness are included in a system with a Dirac spectrum, and, specifically, the interplay of the quantum critical point associated with the semimetal to antiferromagnet (AFM) transition in the clean system with the localizing effects of disorder.

Phenomenologically, this separation of the metal insulator and AFM transitions is reminiscent of the problem in the physics of the disordered *bosonic* Hubbard Hamiltonian [13,14]: the question of whether there could be a direct superfluid to insulator transition, or whether a "Bose Glass" phase always intervenes. This issue was very actively debated over more than a decade [15–22] before finally being settled [23]. Even so, subtleties of the result continued to be explored [24,25]. Our work here marks the first step in addressing similar issues for fermions. We focus on the Anderson-Hubbard model on the honeycomb lattice, a minimal model that includes both disorder and interactions in a 2D Dirac system. The model is solved numerically using the exact determinant quantum Monte Carlo (DQMC) method [26] that treats disorder and correlations on the same footing. Electronic, transport, and magnetic properties are analyzed, resulting in the key findings summarized in the phase diagram Fig. 1. Whereas in the absence of disorder the metal insulator and AFM phase transitions coincide at a common critical coupling [27], an intervening nonmagnetic insulating phase emerges from the quantum critical point with the addition of disorder. Inside this novel nonmagnetic phase, a subtle crossover between two different types of insulators is uncovered.

Model and method—The Anderson-Hubbard model is defined as

$$\hat{H} = -\sum_{\langle \mathbf{ij}\rangle\sigma} t_{\mathbf{ij}}(\hat{c}^{\dagger}_{\mathbf{i}\sigma}\hat{c}_{\mathbf{j}\sigma} + \hat{c}^{\dagger}_{\mathbf{j}\sigma}\hat{c}_{\mathbf{i}\sigma}) - \mu\sum_{\mathbf{i}\sigma}\hat{n}_{\mathbf{i}\sigma} + U\sum_{\mathbf{i}}\left(\hat{n}_{\mathbf{i}\uparrow} - \frac{1}{2}\right)\left(\hat{n}_{\mathbf{i}\downarrow} - \frac{1}{2}\right). \quad (1)$$

$\hat{c}^{\dagger}_{\mathbf{i}\sigma}$ ($\hat{c}_{\mathbf{i}\sigma}$) is the spin-$\sigma$ electron creation (annihilation) operator at site $\mathbf{i}$. $U > 0$ is the interaction strength. $t_{\mathbf{ij}}$ is the hopping integral between two near-neighbor sites $\mathbf{i}$ and $\mathbf{j}$. The chemical potential μ determines the density of the system, and $\hat{n}_{\mathbf{i}\sigma}$ is the number operator. Disorder is introduced through the hopping matrix elements $t_{\mathbf{ij}}$ chosen

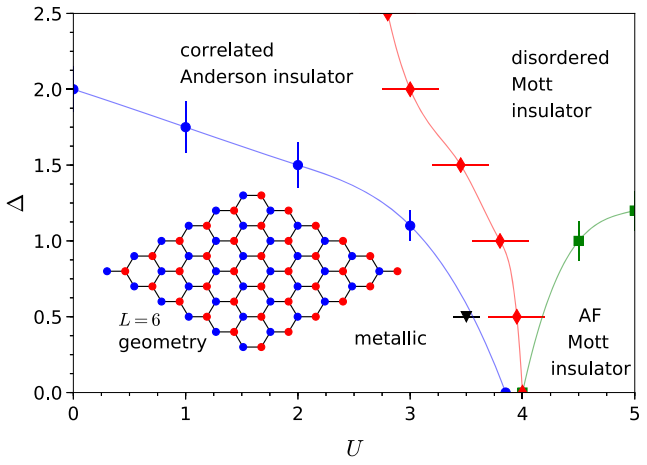

FIG. 1. Phase diagram of the disordered Hubbard model on the honeycomb lattice at half-filling. Δ labels the disorder strength and U represents the local Coulomb repulsion. Phase boundary lines are guides to the eye. The metallic phase boundary is determined by the temperature dependence of the conductivity $\sigma_{\rm dc}$ and the region of long range AFM order by finite size scaling of the AFM structure factor. The (black) triangle point is obtained using the Drude weight data presented in the Supplemental Material [29]. Lines are guides to the eyes. Although these transitions coincide in the clean limit, for nonzero Δ an intermediate, magnetically disordered, insulator phase intervenes. This phase itself contains a transition from Anderson-like to Mott-like insulators. The inset shows the geometry of the $L = 6$ lattice where sublattices are labeled by blue and red colors.

uniformly $P(t_{\mathbf{ij}}) = 1/\Delta$ for $t_{\mathbf{ij}} \in [t - \Delta/2, t + \Delta/2]$, and zero otherwise. The strength of disorder is characterized by Δ. We set $t = 1$ as the energy scale and consider $\mu = 0$, where the disordered system is half-filled and particle-hole symmetric [28].

Within the DQMC approach [26], the Hamiltonian Eq. (1) is mapped onto free fermions coupled to space and imaginary-time dependent Ising fields. The integration over all possible field configurations is carried out by Monte Carlo sampling. The discretization mesh $\Delta\tau$ of the inverse temperature $\beta = 1/T$ was chosen small enough so that the "Trotter errors" are smaller than those associated with the statistical sampling. This approach allows us to compute static and dynamic observables at a given temperature T. Because of the particle-hole symmetry, the system is sign-problem free and the simulation can be performed at large enough β to converge to the ground state. Data reported are obtained on $2L^2$ honeycomb lattices with periodic boundary conditions. The inset of Fig. 1 shows the $L = 6$ geometry. In the presence of disorder, results are averaged over 20 disorder realizations [29]. The error bar reflects both statistical and disorder sampling fluctuations.

To study the possible metal-insulator transition (MIT), we examine the T-dependent dc conductivity computed from the momentum $\mathbf{q}$- and imaginary time τ-dependent current correlation function [34]

$$\sigma_{\rm dc}(T) = \frac{\beta^2}{\pi}\Lambda_{xx}(\mathbf{q} = 0, \tau = \beta/2). \tag{2}$$

Here $\Lambda_{xx}(\mathbf{q}, \tau) = \langle \hat{j}_x(\mathbf{q}, \tau)\hat{j}_x(-\mathbf{q}, 0)\rangle$, and $\hat{j}_x(\mathbf{q}, \tau)$ is the current operator in the x direction. The validity of Eq. (2) has been benchmarked extensively [28,30,34]. For disordered systems, the equation provides a good approximation if the temperature is lower than the energy scale set by the disorder strength Δ [34].

In addition to transport properties, we also examine the charge excitation gap and the antiferromagnetic structure factor at wave vector $\mathbf{Q} = \Gamma$,

$$S_{\rm AFM} = \frac{1}{N_c}\left\langle\!\!\left\langle \left(\sum_{\mathbf{r}\in A}\hat{S}^z_{\mathbf{r}} - \sum_{\mathbf{r}\in B}\hat{S}^z_{\mathbf{r}}\right)^2 \right\rangle\!\!\right\rangle_\Delta . \tag{3}$$

Here N_c is the number of unit cells, A and B are sublattices of the honeycomb lattice, and $\hat{S}^z_{\mathbf{r}}$ is the z component spin operator. The inner (outer) bracket $\langle\ldots\rangle$ denotes Monte Carlo (disorder Δ) average.

Results and discussion—We first demonstrate results for the disorder-free system. Figure 2(a) shows $\sigma_{\rm dc}(T)$ computed on the $L = 12$ lattice across several coupling strengths. Regardless of U, the conductivity increases until the temperature is lowered to $T \gtrsim 0.25$. For $U \leq 3.8$, $d\sigma_{\rm dc}/dT < 0$ and $\sigma_{\rm dc}$ diverges as the temperature is further decreased to the limit $T \to 0$. For $U \geq 4.0$, the $\sigma_{\rm dc}(T)$ curve is concave down and approaches zero with decreasing temperature. This change of low-T behavior in $\sigma_{\rm dc}(T)$ suggests that there is a metal-insulator transition [28]. Given the available data, the estimated MIT critical point is $U_c^\sigma \sim 3.9 \pm 0.1$. To examine the magnetic transition, Fig. 2(b) presents a finite-size scaling study of the AFM spin structure factor $S_{\rm AFM}/N_c$. By extrapolating the data to the thermodynamic limit, we estimate the critical point of the magnetic phase transition to be $U_c^{\rm AFM} \sim 4.0 \pm 0.3$. The critical points coincide and are consistent with previous findings [35].

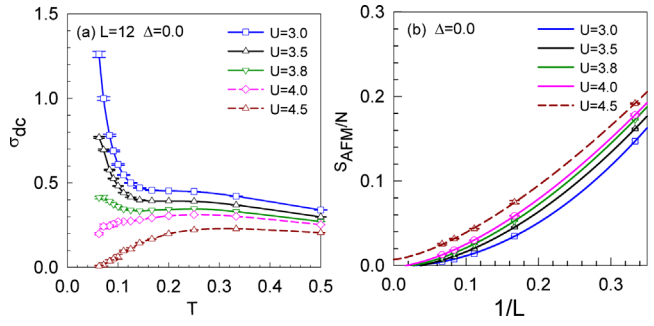

FIG. 2. (a) dc conductivity $\sigma_{\rm dc}$ versus temperature T in the clean limit $\Delta = 0$ computed at various coupling strengths for the $L = 12$ honeycomb lattice. (b) Scaling behavior of the normalized AFM spin structure factor $S_{\rm AFM}/N_c$ at corresponding U values. Solid and dashed lines represent third-order polynomial fits to the data.

Next we move on to the disordered case, presenting transport property results first. We begin the discussion by noting that in disordered graphene and without interactions, electronic transport has been extensively investigated [36–44]. Figure 3 shows $\sigma_{\rm dc}(T)$ computed in a range of disorder strengths at four representative coupling strengths. In panels (a)–(c) of the figure, the low temperature behavior of $\sigma_{\rm dc}$ clearly indicates that there is a disorder-driven metal-insulator transition. For instance, at $U = 1.0$ and $\Delta = 0.5$, the conductivity curve is concave up $d\sigma_{\rm dc}/dT < 0$ for $T \lesssim 0.2$. By the time the temperature drops to $T \sim 0.1$, $\sigma_{\rm dc}(T)$ is increasing rapidly, indicating that the system is metallic. At $\Delta = 2.5$, on the other hand, $\sigma_{\rm dc}(T)$ decreases as the temperature is lowered, and approaches zero as $T \to 0$, suggesting that the system has become insulating. At $U = 1.0$, the metal-insulator transition critical disorder strength is estimated to be $\Delta_c \sim 1.7 \pm 0.2$. Δ_c becomes smaller as U is raised. The critical disorder strengths for the MIT are $\Delta_c \sim 1.5 \pm 0.2$ and 1.1 ± 0.1 for $U = 2.0$ and 3.0, respectively. At $U = 4.0$, the conductivity curve plotted in Fig. 3(d) exhibits an insulating response $d\sigma_{\rm dc}/dT > 0$ and approaches zero as $T \to 0$ for any $\Delta \geq 0.5$. As an independent check of the above findings, we have computed the Drude weight $D(\omega_n)$ in the low Matsubara frequency limit $\omega_n \to 0$ at $\Delta = 0.5$. The data presented in the Supplemental Material [29] point to a MIT at a coupling strength between $U = 3.0$ and 4.0, consistent with transport results.

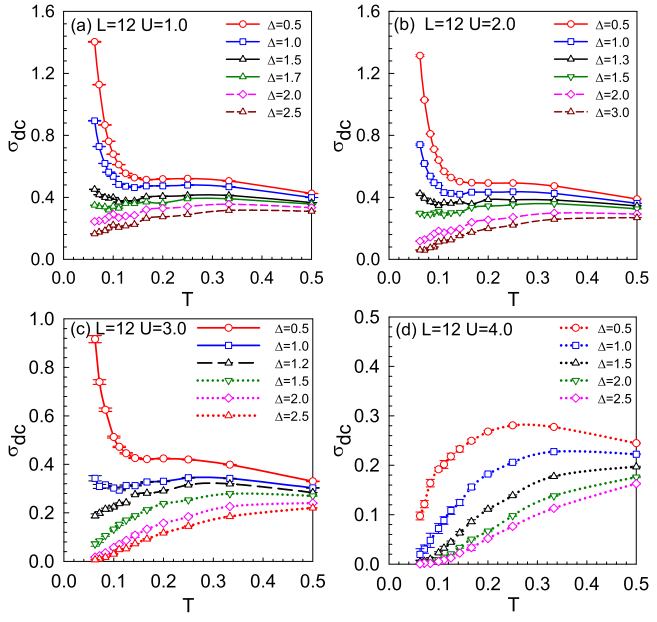

FIG. 3. Temperature dependence of the dc conductivity $\sigma_{\rm dc}$ measured on the $L = 12$ lattice with disorder at (a) $U = 1.0$, (b) $U = 2.0$, (c) $U = 3.0$, and (d) $U = 4.0$. In each figure, lines are guides to the eyes. Metallic and insulating behaviors are indicated by solid and dashed lines, respectively. In panels (a)–(c), the low-T behavior of $\sigma_{\rm dc}$ clearly indicates a disorder-driven metal-insulator transition.

The "metallic" region of the phase diagram Fig. 1 summarizes these transport results. As previously found for the quarter-filled square lattice Hubbard model with bond disorder [28], our data suggest that the onsite Hubbard repulsion can introduce metallic behavior in the 2D honeycomb lattice even at the Dirac point where the density of states is vanishing for $U = 0$.

Another electronic property of interest is the single-particle gap. Without disorder, the half-filled Hubbard model on the honeycomb lattice exhibits a charge (Mott) excitation gap at sufficiently large U [27,35]. The non-interacting Anderson insulator, on the other hand, is gapless at the Fermi level (in the thermodynamic limit) [45,46]. Although the gap is not an order parameter associated with symmetry breaking, it nevertheless can be used to establish the existence of the Mott insulator.

The single-particle gap can be extracted from the density of states; however, here we distinguish between gapped and gapless systems using the charge compressibility $\kappa(\mu) = d\langle\hat{n}(\mu)\rangle/d\mu$ at the Fermi level, where $\langle\hat{n}(\mu)\rangle$ is the average density at chemical potential μ. Results for $\kappa(\mu)$ evaluated at inverse temperature $\beta = 10$ are depicted in Fig. 4 for $L = 12$ with various disorder Δ and coupling strength U combinations. Tuning μ away from half-filling breaks the particle-hole symmetry and leads to a sign problem. However, the problem becomes less severe in the presence of disorder [47], and we are able to obtain accurate data.

In the thermodynamic limit, the compressibility κ of a gapped (gapless) system is vanishing (finite) at $T = 0$.

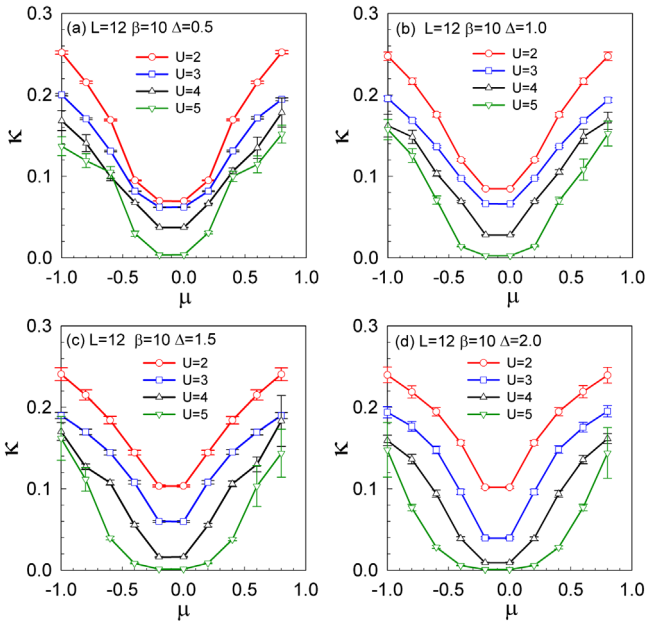

FIG. 4. Charge compressibility κ versus chemical potential μ computed for the linear size $L = 12$ disordered lattice at inverse temperature $\beta = 10$. To distinguish between gapped and gapless phases, we have adopted a finite threshold $\kappa \lesssim 0.04$ deduced from the procedure described in the Supplemental Material [29].

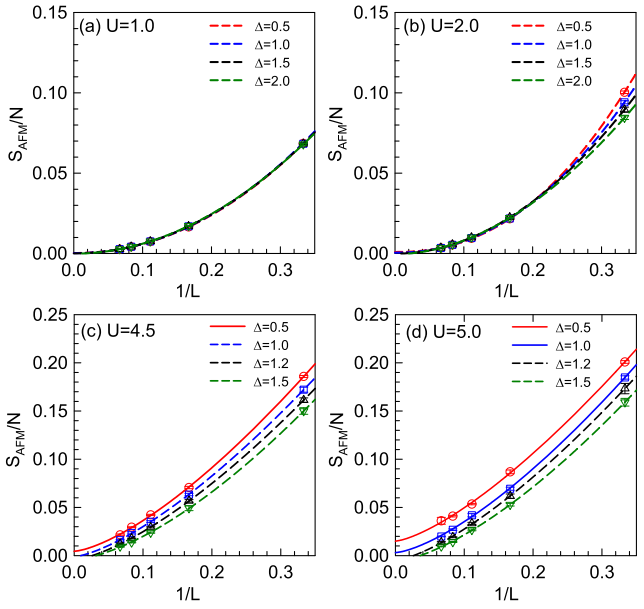

FIG. 5. Finite-size scaling studies of the AFM spin structure factor. Statistical errors of DQMC results are smaller than the symbol size. Lines represent cubic polynomial (in $1/L$) fits to the data. A finite y-axis intercept in the $L \to \infty$ limit indicates the existence of long-range magnetic order. Here again, we have used solid and dashed lines to label magnetically ordered and disordered phases.

However, on finite lattices and at nonzero temperatures, requiring $\kappa = 0$ overestimates the critical coupling due to temperature broadening effects [31]. Analysis of the effect of finite T in the noninteracting limit suggests $\kappa \sim 0.04$ as an appropriate threshold. See Supplemental Material [29].

Figure 4 suggests that for $\Delta = 0.5$, the system becomes incompressible at $U_c \sim 4.0 \pm 0.5$. Increasing the level of randomness, the gap develops at a lower interaction strength, $U_c \sim 3.8 \pm 0.5$ and 3.0 ± 0.5 at $\Delta = 1.0$ and 2.0 respectively. We are not able to pinpoint the exact location where the gap opens at each disorder strength due to the coarse-grained data. Nonetheless, an estimated phase boundary separating Anderson-like (gapless) and Mott-like (gapped) insulators is presented in the phase diagram Fig. 1.

We now consider the effect of randomness on magnetic order. Figure 5 summarizes finite-size scaling studies of the AFM structure factor on lattices up to $2L^2 = 450$ sites. For $U \leq 2.0$, where there is no AFM order in the clean limit, the disorder has essentially no effect [cf. Figs. 5(a) and 5(b)]. At $U > 4.5$, disorder suppresses the long-range AFM order and increases the critical interaction strength. A likely mechanism for the suppression is the tendency towards singlet formation on pairs of sites with large t_{ij} [48]. Based on the extrapolated S_{AFM}/N_c in the thermodynamic limit, a estimated phase boundary for the onset of AFM magnetic order is shown in Fig. 1.

Summary.—We have studied electronic and magnetic properties of a disordered Hubbard model on the honeycomb lattice using the DQMC algorithm. In the absence of disorder, we have verified our results are consistent with previous (higher resolution) findings [27].

In the $U = 0$ limit, the semimetallic phase is driven into a gapless Anderson insulating state by randomness. Switching on the local Coulomb repulsion U, the critical disorder strength for the metal-insulator transition decreases, suggesting that the presence of both disorder and interactions becomes more effective in localizing electrons. At $U > 4.5$, electrons are localized by strong Coulomb correlations in the absence of disorder: the magnetic transition and metal-insulator transition coincide in the clean limit. Our key finding is that adding random disorder reduces the threshold U required for insulating behavior, but increases the U required for antiferromagnetic order. Thus, the magnetic and metal-insulator transitions no longer coincide, and a disordered insulating phase intervenes. Furthermore, within this disordered insulator, there is a transition from an Anderson-like gapless state to a Mott-like gapped phase.

Already, certain unique features of the interplay of disorder and interactions in models with a Dirac dispersion have been noted, including the possibility that disorder might enhance superconductivity for attractive interactions [49]. Our work expands this understanding to repulsive interactions, where similar anomalous effects such as an enhancement of Néel temperature by randomness are known [50] for conventional geometries. Moreover, the reduced critical coupling strength for the metal-insulating transition in the presence of disorder might be relevant for practical applications of honeycomb structural materials such as a low power Mott transistor. Recently, it was shown [51,52] that strongly coupled electron-hole plasma in graphene (dubbed the Dirac fluid) near the charge neutrality point violates the Fermi liquid theory. While our work does not address the issue directly, these are the first steps to future numerical studies of non-Fermi liquid behaviors in Dirac fluids. Finally, we note that there is a renewal of interest in disorder effects in correlated systems using optical lattice experiments. These ultracold atomic systems allow precise control over disorder and coupling parameters, making direct comparisons between experimental data and theoretical predictions feasible [53]. Results reported in this work could be used as guidance in future cold atom experiments.

T. M. thanks CAEP for partial financial support. T. M. and L. F. Z. were supported by NSFCs (Grants No. 11774033, No. 11374034, and No. 11334012), and the Fundamental Research Funds for the Center Universities, Grant No. 2014KJJCB26. We acknowledge computational support from the Beijing Computational Science Research Center (CSRC), the support of HSCC of Beijing Normal University, and phase 2 of the Special Program for Applied Research on Super Computation of the NSFC-Guangdong Joint Fund.

R. T. S. was funded by the Department of Energy (DOE) under Grant No. DE-NA0002908. C.-C. C. acknowledges DOE-LLNL support under Contracts No. DE-AC52-07NA27344 and No. 15-ERD-013.

*ccchang@ucdavis.edu

[1] P. W. Anderson, Phys. Rev. **109**, 1492 (1958).
[2] K. Byczuk, W. Hofstetter, and D. Vollhardt, Int. J. Mod. Phys. B **24**, 1727 (2010).
[3] R. Nandkishore and D. A. Huse, Annu. Rev. Condens. Matter Phys. **6**, 15 (2015).
[4] D. M. Basko, I. L. Aleiner, and B. L. Altshuler, Ann. Phys. (Amsterdam) **321**, 1126 (2006).
[5] M. Z. Hasan and C. L. Kane, Rev. Mod. Phys. **82**, 3045 (2010).
[6] X.-L. Qi and S.-C. Zhang, Rev. Mod. Phys. **83**, 1057 (2011).
[7] S. Raghu, X.-L. Qi, C. Honerkamp, and S.-C. Zhang, Phys. Rev. Lett. **100**, 156401 (2008).
[8] D. Pesin and L. Balents, Nat. Phys. **6**, 376 (2010).
[9] T. Grover and A. Vishwanath, arXiv:1206.1332.
[10] P. Ponte and S.-S. Lee, New J. Phys. **16**, 013044 (2014).
[11] T. Grover, D. N. Sheng, and A. Vishwanath, Science **344**, 280 (2014).
[12] R. Nandkishore, J. Maciejko, D. A. Huse, and S. L. Sondhi, Phys. Rev. B **87**, 174511 (2013).
[13] T. Giamarchi and H. J. Schulz, Phys. Rev. B **37**, 325 (1988).
[14] M. P. A. Fisher, P. B. Weichman, G. Grinstein, and D. S. Fisher, Phys. Rev. B **40**, 546 (1989).
[15] R. T. Scalettar, G. G. Batrouni, and G. T. Zimanyi, Phys. Rev. Lett. **66**, 3144 (1991).
[16] W. Krauth, N. Trivedi, and D. Ceperley, Phys. Rev. Lett. **67**, 2307 (1991).
[17] M. Wallin, E. S. Sorensen, S. M. Girvin, and A. P. Young, Phys. Rev. B **49**, 12115 (1994).
[18] F. Pázmándi, G. Zimányi, and R. Scalettar, Phys. Rev. Lett. **75**, 1356 (1995).
[19] J. K. Freericks and H. Monien, Phys. Rev. B **53**, 2691 (1996).
[20] R. Pai, R. Pandit, H. R. Krishnamurthy, and S. Ramasesha, Phys. Rev. Lett. **76**, 2937 (1996).
[21] J. Kisker and H. Rieger, Phys. Rev. B **55**, R11981 (1997).
[22] I. Herbut, Phys. Rev. Lett. **79**, 3502 (1997).
[23] L. Pollet, N. V. Prokofév, B. V. Svistunov, and M. Troyer, Phys. Rev. Lett. **103**, 140402 (2009).
[24] V. Gurarie, L. Pollet, N. V. Prokofév, B. V. Svistunov, and M. Troyer, Phys. Rev. B **80**, 214519 (2009).
[25] Y. Wang, W. Guo, and A. W. Sandvik, Phys. Rev. Lett. **114**, 105303 (2015).
[26] S. R. White, D. J. Scalapino, R. L. Sugar, E. Y. Loh, J. E. Gubernatis, and R. T. Scalettar, Phys. Rev. B **40**, 506 (1989).
[27] T. Paiva, R. T. Scalettar, W. Zheng, R. R. P. Singh, and J. Oitmaa, Phys. Rev. B **72**, 085123 (2005); S. Sorella, Y. Otsuka, and S. Yunoki, Sci. Rep. **2**, 992 (2012); F. F. Assaad and I. F. Herbut, Phys. Rev. X **3**, 031010 (2013); S. Arya, P. V. Sriluckshmy, S. R. Hassan, and A.-M. S. Tremblay, Phys. Rev. B **92**, 045111 (2015).
[28] P. J. H. Denteneer, R. T. Scalettar, and N. Trivedi, Phys. Rev. Lett. **83**, 4610 (1999).
[29] See Supplemental Material at http://link.aps.org/supplemental/10.1103/PhysRevLett.120.116601 where we have verified that 20 disorder realizations are sufficient for the results to converge and provide details on the number of realizations. The Supplemental Material includes Refs. [30–33].
[30] N. Trivedi, R. T. Scalettar, and M. Randeria, Phys. Rev. B **54**, R3756 (1996).
[31] K.-W. Lee, J. Kuneš, R. T. Scalettar, and W. E. Pickett, Phys. Rev. B **76**, 144513 (2007).
[32] D. J. Scalapino, S. R. White, and S. C. Zhang, Phys. Rev. B **47**, 7995 (1993).
[33] R. K. Pathria, *Statistical Mechanics*, 2nd ed. (Butterworth-Heinemann, Oxford, 1996), Chap. 8, p. 197.
[34] N. Trivedi and M. Randeria, Phys. Rev. Lett. **75**, 312 (1995).
[35] Y. Otsuka, S. Yunoki, and S. Sorella, Phys. Rev. X **6**, 011029 (2016).
[36] I. L. Aleiner and K. B. Efetov, Phys. Rev. Lett. **97**, 236801 (2006).
[37] E. Fradkin, Phys. Rev. B **33**, 3257 (1986).
[38] N. H. Shon and T. Ando, J. Phys. Soc. Jpn. **67**, 2421 (1998).
[39] H. Suzuura and T. Ando, Phys. Rev. Lett. **89**, 266603 (2002).
[40] Y. Zheng and T. Ando, Phys. Rev. B **65**, 245420 (2002).
[41] T. Ando, Y. Zheng, and H. Suzuura, J. Phys. Soc. Jpn. **71**, 1318 (2002).
[42] D. V. Khveshchenko, Phys. Rev. Lett. **97**, 036802 (2006).
[43] A. F. Morpurgo and F. Guinea, Phys. Rev. Lett. **97**, 196804 (2006).
[44] E. McCann, K. Kechedzhi, V. I. Fal'ko, H. Suzuura, T. Ando, and B. L. Altshuler, Phys. Rev. Lett. **97**, 146805 (2006).
[45] P. W. Anderson, Rev. Mod. Phys. **50**, 191 (1978).
[46] D. Thouless, Int. J. Mod. Phys. B **24**, 1507 (2010).
[47] T. Paiva, E. Khatami, S. Yang, V. Rousseau, M. Jarrell, J. Moreno, R. G. Hulet, and R. T. Scalettar, Phys. Rev. Lett. **115**, 240402 (2015).
[48] M. Enjalran, F. Hebert, G. G. Batrouni, R. T. Scalettar, and S. Zhang, Phys. Rev. B **64**, 184402 (2001).
[49] I.-D. Potirniche, J. Maciejko, R. Nandkishore, and S. L. Sondhi, Phys. Rev. B **90**, 094516 (2014).
[50] M. Ulmke, V. Janis, and D. Vollhardt, Phys. Rev. B **51**, 10411 (1995).
[51] J. Crossno, J. K. Shi, K. Wang, X. Liu, A. Harzheim, A. Lucas, S. Sachdev, P. Kim, T. Taniguchi, K. Watanabe, T. A. Ohki, and K. C. Fong, Science **351**, 1058 (2016).
[52] A. Lucas, J. Crossno, K. C. Fong, P. Kim, and S. Sachdev, Phys. Rev. B **93**, 075426 (2016).
[53] M. Pasienski, D. McKay, M. White, and B. DeMarco, Nat. Phys. **6**, 677 (2010); S. S. Kondov, W. R. McGehee, W. Xu, and B. DeMarco, Phys. Rev. Lett. **114**, 083002 (2015); M. Schreiber, S. S. Hodgman, P. Bordia, H. P. Lüschen, M. H. Fischer, R. Vosk, E. Altman, U. Schneider, and I. Bloch, Science **349**, 842 (2015); P. Bordia, H. P. Lüschen, S. S. Hodgman, M. Schreiber, I. Bloch, and U. Schneider, Phys. Rev. Lett. **116**, 140401 (2016).